frontiers in Energy Research

ORIGINAL RESEARCH
published: 24 November 2021
doi: 10.3389/fenrg.2021.780008

Size Effect of Fe_3O_4 Nanoparticles on Magnetism and Dispersion Stability of Magnetic Nanofluid

Fang Chen[1,2], *Nasir Ilyas*[1], *Xiaobing Liu*[2], *Zhenggui Li*[2], *Shengnan Yan*[2] *and Hao Fu*[1]*

[1]School of Physics, University of Electronic Science and Technology of China, Chengdu, China, [2]Key Laboratory of Fluid and Power Machinery, Ministry of Education, Xihua University, Chengdu, China

It is well known that magnetic nanofluids are widely applied in various fields ranging from heat transfer to miniature cooling, and from damping to sealing, due to the mobility and magnetism under magnetic field. Herein, the PFPE-oil based magnetic nanofluids with superior magnetization and dispersion stability were obtained *via* regulating reaction temperature. The structures of particles were characterized by X-ray diffraction (XRD) and transmission electron microscopy (TEM). The size effects of particles on the magnetism and coating effect of particles, and on the stability and saturation magnetization of the fluids were characterized by Fourier transform infrared spectroscopy (FTIR), thermogravimetric analysis (TGA), vibrating sample magnetometer (VSM) and density instrument, respectively. The results indicate that the impurity phase FeOOH only appear in the sample prepared at 18°C and the average size of Fe_3O_4 nanoparticles reduces from 120 to 20 nm with raising reaction temperature. The saturation magnetization of Fe_3O_4 particles increases firstly and then reduces with increasing particle size, which is affected by the thickness of magnetic dead layer and impurity phase FeOOH. The Fe_3O_4 particles could be chemically coated by PFPE-acids, and the coated mass is a little affected by particle size. The stability of the nanofluids lowers while the saturation magnetization increases firstly and then decrease with increasing particle size. At reaction temperature of 60°C, Fe_3O_4 particles of 25 nm and the nanofluids with superior stability and saturation magnetization were obtained. Our results indicate that the control of nanoparticles size by regulating reaction temperature can be a useful strategy for preparing magnetic nanofluids with desirable properties for various potential applications.

Keywords: Fe_3O_4 nanoparticle size, magnetic nanofluids, magnetism, dispersion stability, heat transfer

OPEN ACCESS

Edited by:
Mohsen Sharifpur,
University of Pretoria, South Africa

Reviewed by:
Iskander Tlili,
Majmaah University, Saudi Arabia
Yi Jin,
Jiangsu Jinhe Energy Technology Co. Ltd., China

***Correspondence:**
Hao Fu
Fuhao@12uestc.edu.cn

Specialty section:
This article was submitted to Process and Energy Systems Engineering, a section of the journal Frontiers in Energy Research

Received: *20 September 2021*
Accepted: *08 November 2021*
Published: *24 November 2021*

Citation:
Chen F, Ilyas N, Liu X, Li Z, Yan S and Fu H (2021) Size Effect of Fe_3O_4 Nanoparticles on Magnetism and Dispersion Stability of Magnetic Nanofluid. Front. Energy Res. 9:780008. doi: 10.3389/fenrg.2021.780008

INTRODUCTION

The nanofluids are colloidal suspensions composed of various nanoparticles (Al_2O_3, TiO_2, ZnO, CuO, SiO_2, Fe_3O_4, etc.) (Shahrul et al., 2016; Nayak et al., 2020; Aldabesh et al., 2021; Awan et al., 2021; Iskander, 2021; Khan et al., 2021; Tlili et al., 2021), and these particles have different characteristics, for example, ZnO has the highest thermal conductivity, SiO_2 has lowest thermal conductivity, Fe_3O_4 has magnetism and enhancement of thermal conductivity (Lemes et al., 2017). Magnetic nanofluids have magnetism and mobility under a magnetic field, and thus, which are called "smart materials" and widely applied in many fields, such as heat transfer, miniature cooling,

damping, biomedicine and sealing (Yadav et al., 2013; Akbar et al., 2016; Shahsavar et al., 2016; Chen et al., 2018; Chen et al., 2019).

The performance and applications of magnetic nanofluids depend on their stability, which is related to the proper dispersion of nanoparticles (Chen et al., 2016a; Colla et al., 2012; Aishwarya et al., 2013; Mabood and Akinshilo, 2021). Control of the pH value of suspension, or addition of surfactants, aim to change the surface properties of suspended nanoparticles to avoid the formation of the clusters and achieve a stable suspension (Socoliuc and Vékás, 2014). Most of the studies on the magnetism and stability of magnetic nanofluids are carried out in nanofluids with particle size >20 nm, such suspensions are less stable, due to strong dependence of particle size d on the sedimentation velocity $V \propto d^2$ (Mahbubul, 2019).

However, the high saturation magnetization of magnetic nanofluids is needed in various applications, such as big gap sealing and biomedicine (Sharifi et al., 2012; Yang et al., 2013). The conventional ferrofluids possess low saturation magnetization due to their small average particle size (i.e., ~10 nm) and the differences of particle morphology and types of magnetic component (López-López et al., 2012). Even though some magnetorheological fluids contain larger average particle size (i.e., ~ 1 μm) with higher saturation magnetization (Tang, 2011), they exhibit unsatisfied dispersion stability compared to ferrofluids (Chen et al., 2021). Therefore, the two critical parameters, saturation magnetization and stability, must be considered simultaneously for different nanofluids application occasions.

It is well known that the size of magnetic nanoparticles has a great impact on the electronic, optical and magnetic properties compared with their bulk counterparts. Particularly, saturation magnetization can be well-tuned by modifying their size using different synthesis approaches. The Fe_3O_4 particles with size between 67 and 143 nm were obtained *via* regulating the ion concentration through an one-pot method, and the saturation magnetization of particles increases from 63.0 emu/g to 68.9 emu/g (Dong et al., 2016). The Fe_3O_4 particles with average size in range of 21–123 nm were obtained by regulating reaction time *via* hydrothermal process and the saturation magnetization also increases from 77.9 emu/g to 92.5 emu/g (Ozel et al., 2015). Li J. H. prepared the Fe_3O_4 nanocrystals by thermal decomposition, the range of particle size is from 4 to 12 nm and the saturation magnetization of Fe_3O_4 increase from 25 emu/(g Fe) to 102 emu/(g Fe) (Jun et al., 2005). Particle size has a strong effect on the magnetic properties of nanoparticles, and which turned out to be caused by the magnetic dead layer. In addition, Brownian motion provides a physical foundation for stability in magnetic nanofluids applications, also determined by the magnetic particle size (Fannin and Charles, 2001). The magnetic nanoparticles of small size are beneficial to the stability of magnetic nanofluids. Therefore, it is important to tune the magnetic property and size of nanoparticles in terms of saturation magnetization and stability of magnetic nanofluids.

The aims of this paper are to prepare Fe_3O_4 nanoparticles with different sizes and optimize the saturation magnetization of magnetic nanofluids with high dispersion stability, thus to facilitate their applications in thermal conductivity, big gap sealing and other occasions.

EXPERIMENTAL

Preparation of Fe_3O_4 Nanoparticles and PFPE-Oil Based Magnetic Nanofluids

Briefly, ferrous sulfate ($FeSO_4{\cdot}7H_2O$), sodium hydroxide (NaOH), sodium nitrate ($NaNO_3$), hydrochloric acid (HCl), ethyl alcohol (C_2H_5OH), PFPE-acids (C_3F_7O-$(C_3F_6O)_n$-$C_3F_4O_2H$, of which n is about 10) and PFPE-oils [F-$(C_3F_6O)_n$-C_2F_5, of which n is about 27] were all purchased from a local chemical supplier. All chemicals were of analytical grade and were used without any further purification.

First, the NaOH (0.5 M, 20 g), $NaNO_3$ (0.1 M, 8.5 g), and $FeSO_4{\cdot}7H_2O$ (0.1 M, 27.8 g) were dissolved in 1,000 ml ultrapure water by stirring at room temperature, respectively. The solutions containing sodium ions were mixed and added to the solution containing iron ions, and then a stirring process was applied for 5 min when the stirring speed was 100 r/min. After that, the oxidation precipitation reaction was carried out at various temperatures (i.e., 18°C, 35°C, 45°C, 60°C, 80°C) for 24 h, respectively. And then, the pH of reaction solutions was adjusted to be ~7 by dropping in HCl, and then PFPE-acids (6 g) were added and mechanical stirring was carried out to coat the Fe_3O_4 nanoparticles. These coated nanoparticles were washed with deionized water (DIW) and C_2H_5OH until the pH of the solution was neutralized. Once the solution was neutralized, these nanoparticles were dried and subjected to characterizations.

Finally, these Fe_3O_4 nanoparticles were dispersed in PFPE-oil for preparing a series of magnetic nanofluids possessing different average particle sizes. The solid concentration in the magnetic nanofluids remains 10 wt.%. **Figure 1** presents a schematic illustration of the preparation process of magnetic nanofluids.

Characterization Methods

X-ray diffraction (XRD) analysis was performed on a DX-2700X X-ray diffractometer equipped with Cu Kα (λ = 0.154 nm) radiation. Scans were made from 10° to 80° at the rate of 0.085 deg./s. High-resolution transmission electron microscopy (TEM: JEM-2000EX) was employed to study the microstructure and size dispersion of synthesized Fe_3O_4 nanoparticles. A vibrating sample magnetometer (VSM, Lake Shore 7410) was used for the magnetic characterization of nanoparticles and ferrofluids at an external magnetic field ranging from -2.5×10^4 Oe to $+2.5\times10^4$ Oe at 25°C. Fourier Transform Infrared Spectrometer (FTIR, Nicolet iS10) spectra were recorded over the wavenumber range of 400–4,000 cm^{-1} to investigate the interactions between surfactants and magnetic nanoparticles. Thermogravimetric analysis (TGA) of coated nanoparticles was performed using a TGA, TG209F1 analyzer, from RT to 600°C with a heating rate of 10°C/min in an argon atmosphere. A densimeter (ST-300GM) was used to measure the density of a magnetic nanofluids. All the magnetic nanofluids samples were centrifuged for two hours at 5,000 rpm to measure the magnetic nanofluids saturation magnetization and the stability.

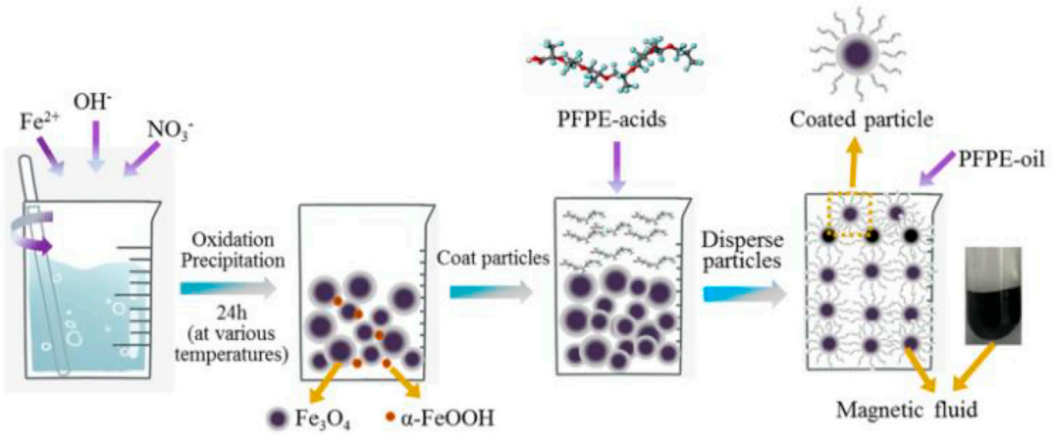

FIGURE 1 | Schematic illustration of the preparation process for Fe_3O_4 nanoparticles dispersed in PFPE oil-based magnetic nanofluids.

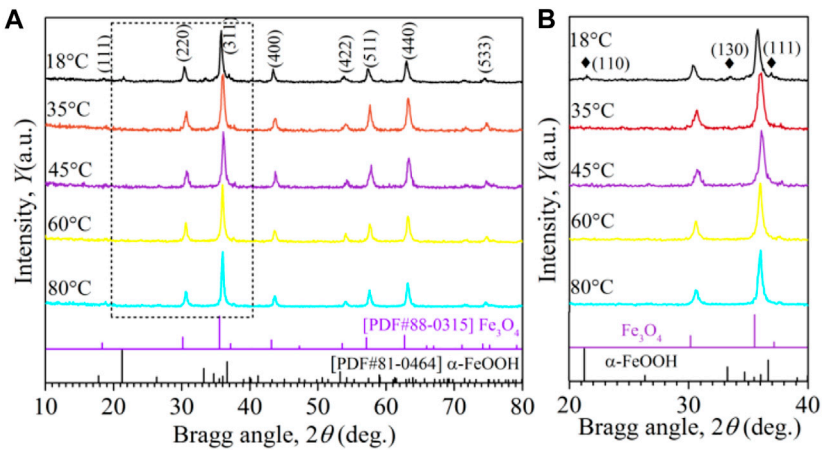

FIGURE 2 | (A) XRD profiles of the samples prepared at different reaction temperatures, **(B)** the extended XRD profiles from 20 to 40°.

RESULTS AND DISSCUSSION

The Structures of Nanoparticles

Figure 2 shows the XRD patterns of the Fe_3O_4 nanoparticles prepared at various reaction temperatures. The diffraction peaks of Fe_3O_4 nanoparticles correspond to the planes, such as (111), (220), (311), (400), (422), (511), (440), and (533) that can be unambiguously observed [PDF#88-0315] (Vasilescu et al., 2018; Kamali et al., 2016). With the increasing temperature, the peaks intensity and full-wave half maximum (FWHM) were observed, indicating that Fe_3O_4 nanoparticles contain a significant volume fraction of single-phase crystalline structure. On the other hand, the Fe_3O_4 nanoparticles prepared at room temperature (RT), the dual-phase structure consisting of the Fe_3O_4 spinel phase seemed dominant (Yang et al., 2012) and an impurity phase as well. From the extended XRD profiles in **Figure 2B**, the diffraction peaks at 2θ values of 21.24, 33.24, and 36.66 correspond to the reflections of the (110), (130), and (111) planes of α-FeOOH (PDF#81-0464), and which can be identified from these three peak planes marked with black diamond symbols. These results suggest that in the synthesis process of Fe_3O_4, the intermediate product α-FeOOH formed when the synthesis process was carried out at RT. At higher oxidation reaction temperatures, the intermediate product α-FeOOH are vanished, indicating that α-FeOOH is wholly converted to Fe_3O_4 material (Altman et al., 2004; Jia and Gao, 2007; Li et al., 2011).

Figures 3A–E shows the TEM images and size distributions of the Fe_3O_4 nanoparticle synthesized at different temperatures. It can be seen that all the nanoparticles are nearly quadrilateral in shape. The average size and the distribution span of the nanoparticles decrease with the increase of temperature.

In general, the increase of reaction temperature is conductive to the growth of particles. Here, the estimated average nanoparticles size synthesized at oxidation reaction temperature varied from room temperature (RT) to 80°C is 118.7, 69.9, 49.3, 24.6, and 20.1 nm, particle size decreases

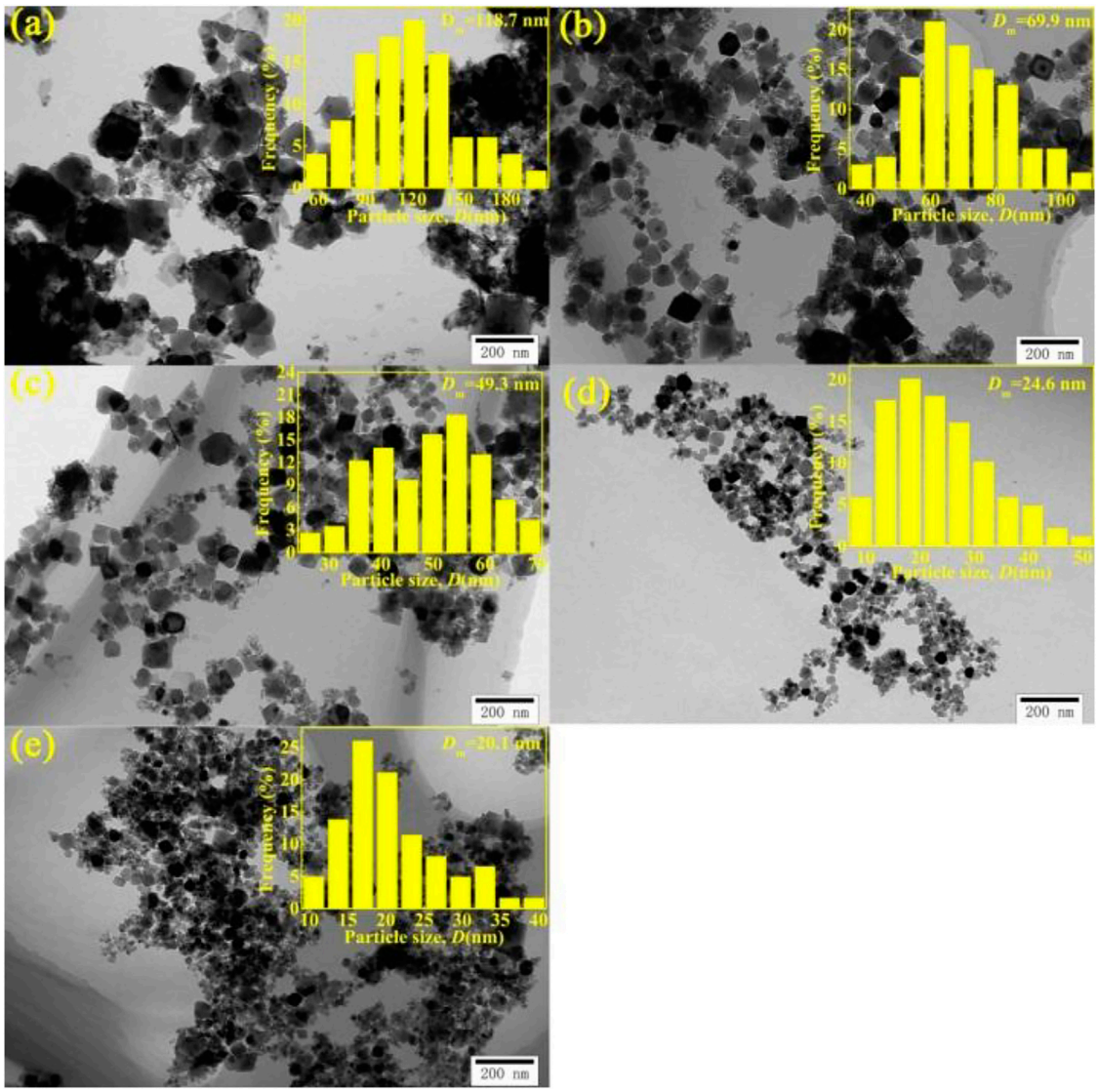

FIGURE 3 | TEM images and size distributions of Fe_3O_4 nanoparticles prepared at different temperatures: **(A)** 18°C (RT), **(B)** 35°C, **(C)** 45°C, **(D)** 60°C, and **(E)** 80°C, and the insets represent of particle sizes.

with increasing temperature. The similar effect of temperature on particle size has appeared and has been well revealed by Wang W. (Wang et al., 2008). and K. Nishio (Nishio et al., 2007). These studies revealed that the particle size could be effectively controlled at the nucleation stage. When the total volume of all nanoparticles is constant, the volume of one particle is inversely proportional to the final number of nanoparticles. The final number of nanoparticles could be expressed by the equation (**Eq. 1**) (Sugimoto et al., 1998)

$$n_+^{\infty} = Q_0 V_m / v_+ \quad (1)$$

Where, n_+^{∞} is the number of nanoparticles, Q_0 the rate of monomer provided, V_m the molar volume of solids and v_+ indicates the volume growth rate of a single particle. When the increased effect caused by temperature on Q_0 is greater than the effect on v_+, n_+^{∞} increases and the final size of nanoparticles decreases. And therefore, the increase of the oxidation reaction temperature causes the decrease of particle size.

The Magnetism of Nanoparticles

In order to analyze the magnetic properties of Fe_3O_4 nanoparticles synthesized at different temperatures, magnetic field-magnetization (H-M_s) characteristics are measured, as shown in **Figure 4A**. It should be noted that the saturation magnetizations are 81.7, 89.8, 94.9, 82.8, and 71.0 emu/g for the samples synthesized at 18, 35, 45, 60, 80°C, respectively. Besides, the inset in **Figure 4A** shows that the coercivities of nanoparticles are small and fall in the interval of 75 through 125 Oe. On the other hand, the Fe_3O_4 particle size decreases with increasing reaction temperature, and thus, the saturation magnetization of nanoparticles decreases is shown in **Figure 4B**.

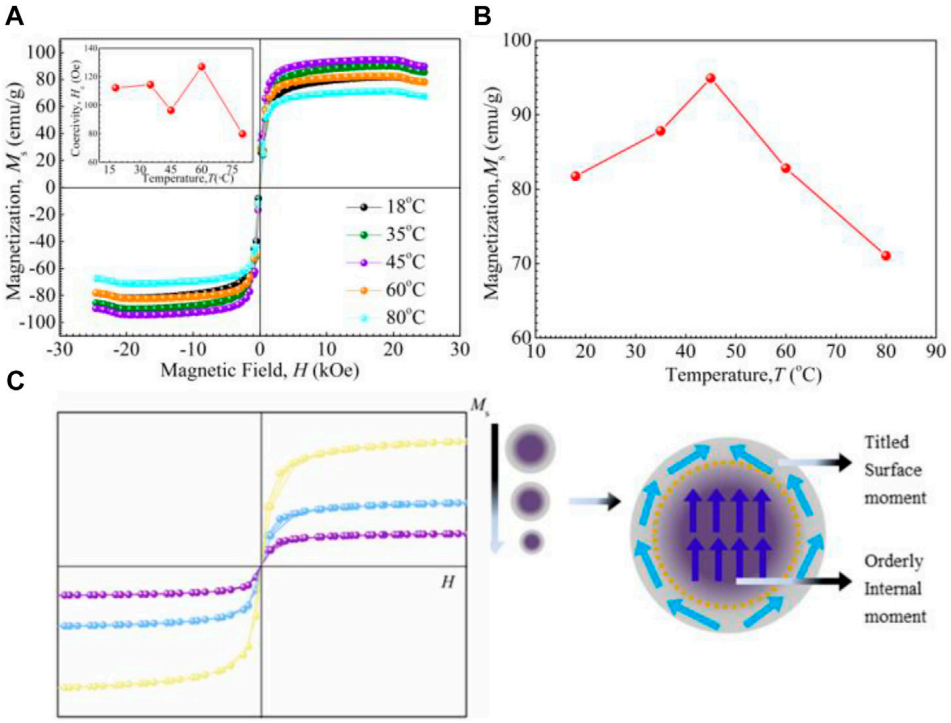

FIGURE 4 | Magnetic properties of Fe_3O_4 nanoparticles prepared at different temperatures: **(A)** hysteresis loops, **(B)** preparation temperature dependence of magnetization M_s, **(C)** schematic illustration of the moment alignment of a magnetic nanoparticle.

TABLE 1 | Particle sizes and magnetic parameters of Fe_3O_4 nanoparticles prepared at different temperatures.

Temperature, T (°C)	Size interval, D (nm)	Average size, D_m (nm)	Magnetization, M_s (emu/g)	Coercivity, H_c (Oe)
18	60–190	118.7	81.7	112.1
35	40–110	69.9	89.8	114.3
45	20–70	49.3	94.9	96.4
60	10–50	24.6	82.8	126.9
80	10–40	20.1	71.0	80.0

The variation in magnetic parameters, such as saturation magnetization and coherence to average nanoparticles size are summarized in **Table 1**. From these results, it could be concluded that the nanoparticles synthesized at RT are of superparamagnetic-like materials, which has low saturation magnetization and due to the presence of impurity phase α-FeOOH with low magnetization. In contrast, the Fe_3O_4 particle size decreases with increasing reaction temperature, and thus, the saturation magnetization of nanoparticles decreases (Aslibeiki et al., 2012). **Figure 4C** illustrated the alignment of magnetic moments in nano-sized magnetic materials. The outer moments go around the surface layer instead of aligning with the externally applied field, not the same as in the core. Some moments offset in magnitude and decrease the total magnetization (Mathew and Juang, 2007). Because of this, generally, the outer surface is named as a magnetic dead layer. It has been reported that the magnetic dead layer arises from the destruction of the Fe-O-Fe chain physically (Poddar et al., 2005). The relationship between the saturation magnetization and particle size could be well defined by equation (**Eq. 2**) (Tang et al., 1991)

$$M_{sn} = M_{sb}(1 - 6t/D) \quad (2)$$

Where, M_{sb} and M_{sn} are the saturation magnetization of bulk and nanomaterials, respectively, t is the thickness of the magnetic dead layer and D is the particle size. It is well known that increasing particle size is a useful method to increase the saturation magnetization of nanoparticles. From the preceding analysis, it can be understood that the nanoparticle prepared at 45°C has the maximum saturation magnetization of 94.9 emu/g compare with that of bulk Fe_3O_4 due to the absence of the secondary phase and relatively large particle size. All the nomenclatures used in the paper are shown in **Table 2**.

TABLE 2 | All the nomenclatures used in the paper.

Symbol	Physical asset	Unit
D	Particle size	nm
θ	Bragg angle	deg.
H_c	Coercivity	Oe
H	Magnetic Field	kOe
T' (%)	Transmittance	—
T	Temperature	°C
m (%)	Mass loss	—
M_s	Magnetism	emu/g
ρ	Density	g/cm^3
D_m	Average size	nm

The Coated Effect of PFPE-Acid on the Nanoparticles

The FTIR curves of PFPE-acid and Fe_3O_4 nanoparticles coated with PFPE-acid were studied to gain insight into the coated effect of particles. **Figure 5A** shows that the peak located at 563.1 cm^{-1} can be attributed to the Fe-O bond vibrations in Fe_3O_4 (Li et al., 2007). Also, the peaks centered at 1,238.1, 1,134.0, 1,307.5, and 983.5 cm^{-1} confirm the existence of C-F, CF_2, CF_3, and C-O-C bonds, respectively (Ma et al., 2003). The stretching vibrations of C=O from COOH in the PFPE-acid shift from 1777.3 cm^{-1} to 1,685.5 cm^{-1} in coated Fe_3O_4 nanoparticles using PFPE-acid, which may be due to the red-shift effect of the covalent bonding with the bare charge on nanoparticles (Chen et al., 2016b). From these results, it can be concluded that the PFPE-acid is chemically adsorbed on the surface of Fe_3O_4 nanoparticles with various particle sizes in the range of 20–120 nm.

Furthermore, TGA measurements are taken to further confirm the coating mass. **Figure 5B** shows the weight loss of nanoparticles with respect to temperature. Significant mass is decreased between 200 and 400°C, which may be caused by the decomposition of coated PFPE-acid. In contrast, above the 400°C, no mass loss is detected. As shown in the inset, the loss in mass is calculated, ranging between 32 wt% and 37 wt%, which suggests that the effect of nanoparticle size on the coated mass is insignificant. When chemically coated enough PFPE-acids, some excessive PFPE-acids will further be coated physically. Too much PFPE-acids coated on the nanoparticles will reduce the saturation magnetization and stability of the nanofluids, while less PFPE-acids will reduce the stability of the fluids. (Chen et al., 2018).

The Stability and Magnetism of the Fluids

Following investigations of saturation magnetization and weight loss effect of PFPE-acids and coated Fe_3O_4 nanoparticles, we further investigate the stability of Fe_3O_4 nanoparticles dispersed PFPE-oil based magnetic nanofluids. For this, Fe_3O_4 magnetic nanoparticles coated with PFPE-acid were dispersed in PFPE-oil to form magnetic nanofluids. The stability of the magnetic nanofluids is measured in terms of saturation magnetizations and densities before and after the centrifugation process. For this, all the samples were centrifuged for two hours at 5,000 rpm, and the centrifugal parameters are enough for the sedimentation of agglomerated particle and hence sufficiently characterizing the stability of the magnetic nanofluids. Temperature has obvious effect on particle size, and thus which will further influence the saturation magnetization and density of the magnetic nanofluids, fluid samples were taken from the upper part in centrifuge tubes. Before and after being centrifuged, the magnetic nanofluids were always black and without visible stratification. **Figure 5** shows that the magnetizations are 0.56, 1.95, 4.55, 5.96, 5.91 emu/g for the magnetic nanofluids samples before centrifuging with average nanoparticles size of 118.7, 69.9, 49.3, 24.6, and 20.1 nm at 18, 35, 45, 60, and 80°C, respectively. In addition, considering the concentration of 10 wt% of the magnetic nanoparticles in the magnetic nanofluids, the theoretical magnetizations for the samples are 8.17, 8.98, 9.49, 8.28, and 7.10 emu/g, respectively. The decrease in the magnetization for the samples before centrifuging can be ascribed to precipitation of the large particle sizes of the magnetic nanoparticles (**Table 1**). After adding the Fe_3O_4 nanoparticles into the PFPE-oil, some nanoparticles with large size and uneven coating with PFPE-acid precipitate directly and cause the reduction in magnetization. Also, with increasing the average sizes of magnetic nanoparticles, magnetization increases and tends to be stable at temperatures above 60°C. The reduction in the particle size is responsible for this tendency. The magnetization curve shows the same pattern after the centrifugation process, but the magnetization is observed to decrease further. From these results, it can be understood that further sedimentation during centrifuging occurs because of particle aggregation.

Figure 6 also shows that the densities of the surface fluids before and after centrifugation vary close to magnetization. The

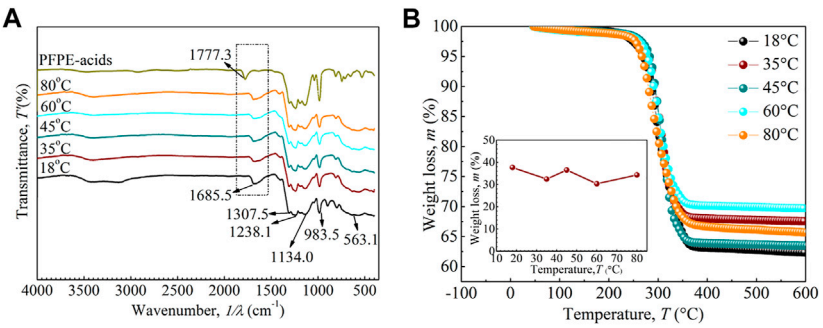

FIGURE 5 | (A) FTIR curves of PFPE-acids and coated Fe_3O_4 nanoparticles with different particle sizes, **(B)** TGA curves of Fe_3O_4 nanoparticles coated with PFPE-acids.

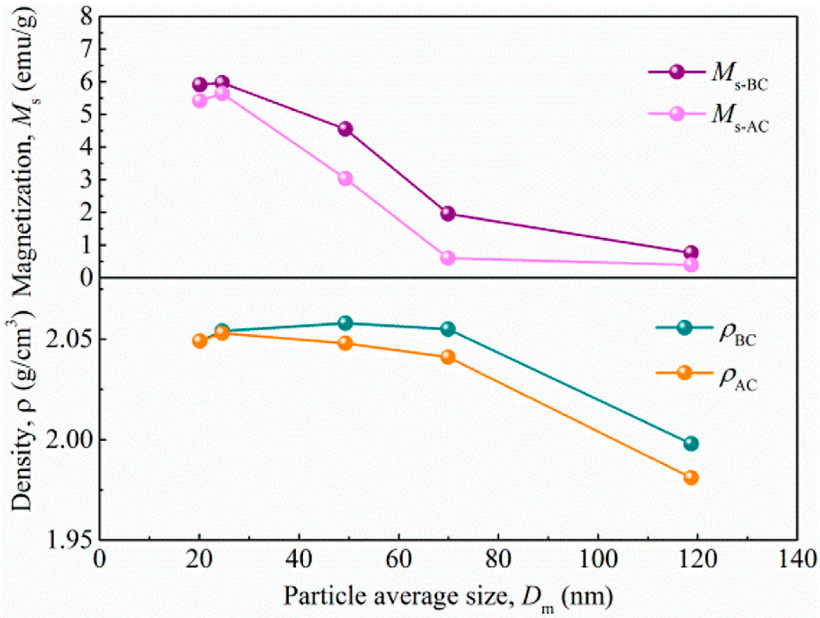

FIGURE 6 | Average sizes of the Fe_3O_4 nanoparticles dependence of the magnetization, density and the stability of the magnetic nanofluids. The subscripts AC and BC represent the samples before and after centrifuging, respectively.

sedimentation of nanoparticles in the magnetic nanofluids can be restrained by hydraulic resistance, and the sedimentation velocity could be obtained by the Stokes equation (**Eq. 3**) (Amirat and Hamdache, 2009)

$$v = \frac{\left(\rho_{N_p} - \rho_{N_c}\right) g d_p^2}{18\eta_c} \tag{3}$$

Where, ρ_{N_c} is the density of a base liquid, ρ_{N_p} the density of particle Fe_3O_4, η_c the dynamic viscosity, d_p the average particle size, and g the acceleration due to gravity. This equation indicates the sedimentation velocity decreased with an increase in viscosity of base liquid and a decrease in the density deviation between the base liquid and the magnetic particle. In addition, the sedimentation velocity increases significantly with the increase of particle size d_p. The increase in particle size is advantageous to increase the saturation magnetization of the fluids while it is disadvantageous to the magnetic nanofluids' stability. Obviously, the optimum preparation temperature should be 60°C, considering the positive contribution of particle size to magnetization and the negative contribution to the magnetic nanofluids' stability.

CONCLUSION

In this study, Fe_3O_4 nanoparticles dispersed into the magnetic nanofluids were prepared. Fe_3O_4 nanoparticles were synthesized by regulating the reaction temperature, and their structural and morphological characteristics were analyzed. It is observed that the saturation magnetization of the nanoparticles first decreased and then increased with rising reaction temperature due to the appearance of impurity and the increase of nanoparticle size. Furthermore, the stability of the prepared magnetic nanofluids decreases when its saturation magnetization increases with the increasing size of the nanoparticles. The magnetic nanofluids with superior stability and magnetization could be obtained with Fe_3O_4 nanoparticles of 25 nm and when the reaction temperature is 60°C.

DATA AVAILABILITY STATEMENT

The original contributions presented in the study are included in the article/Supplementary Material, further inquiries can be directed to the corresponding author.

AUTHOR CONTRIBUTIONS

Conceptualization, FC; investigation, NI; supervision, XL, and ZL, and HF; project administration, SY. All authors have read and agreed to the published version of the manuscript.

FUNDING

This research was financially supported by National Natural Science Foundation of China (No. 52079118) and Key Research and Development Plan of Sichuan province (No. 2020YFH0135).

REFERENCES

Aishwarya, V., Suganthi, K. S., and Rajan, K. S. (2013). Transport Properties of Nano Manganese Ferrite-Propylene Glycol Dispersion (Nanofluids): New Observations and Discussion. *J. Nanopart. Res.* 15 (7), 1–14. doi:10.1007/s11051-013-1774-3

Akbar, N. S., Kazmi, N., Tripathi, D., and Mir, N. A. (2016). Study of Heat Transfer on Physiological Driven Movement with CNT Nanofluids and Variable Viscosity. *Comp. Methods Programs Biomed.* 136, 21–29. doi:10.1016/j.cmpb.2016.08.001

Aldabesh, A., Hussain, M., Khan, N., Riahi, A., Khan, S. U., and Tlili, I. (2021). Thermal Variable Conductivity Features in Buongiorno Nanofluid Model between Parallel Stretching Disks: Improving Energy System Efficiency. *Case Stud. Therm. Eng.* 23, 100820. doi:10.1016/j.csite.2020.100820

Altman, I. S., Jang, Y.-H., Agranovski, I. E., Yang, S., and Choi, M. (2004). Stabilization of Spinel Structure during Combustion Synthesis of Iron Nanooxides. *J. Nanopart. Res.* 6, 633–637. doi:10.1007/s11051-004-5763-4

Amirat, Y., and Hamdache, K. (2009). Weak Solutions to the Equations of Motion for Compressible Magnetic Fluids. *J. de Mathématiques Pures Appliquées* 91, 433–467. doi:10.1016/j.matpur.2009.01.015

Aslibeiki, B., Kameli, P., Manouchehri, I., and Salamati, H. (2012). Strongly Interacting Superspins in Fe3O4 Nanoparticles. *Curr. Appl. Phys.* 12, 812–816. doi:10.1016/j.cap.2011.11.012

Awan, A. B., Zubair, M., Memon, Z. A., Ghalleb, N., and Tlili, I. (2021). Comparative Analysis of Dish Stirling Engine and Photovoltaic Technologies: Energy and Economic Perspective. *Sustainable Energ. Tech. Assessments* 44, 101028. doi:10.1016/j.seta.2021.101028

Chen, B.-Y., Qiu, J.-H., and Feng, H.-X. (2016). Synthesis and Application of Bilayer-Surfactant-Enveloped Fe3O4 Nanoparticles: Water-Based Bilayer-Surfactant-Enveloped Ferrofluids. *Int. J. Miner Metall. Mater.* 23, 234–240. doi:10.1007/s12613-016-1231-2

Chen, F., Liu, X., Li, Z., Yan, S., Fu, H., and Yan, Z. (2021). Investigation of the Rheological Properties of Zn-Ferrite/Perfluoropolyether Oil-Based Ferrofluids. *Nanomaterials* 11 (10), 2653. doi:10.3390/nano11102653

Chen, F., Liu, Y., and Yan, Z. (2018). Influence of Various Parameters on the Performance of superior PFPE-Oil-Based Ferrofluids. *Chem. Phys.* 513, 67–72. doi:10.1016/j.chemphys.2018.05.011

Chen, F., Sun, C., Li, X. H., Zhou, Q. R., Yan, Z. Q., and Li, J. (2019). Splitting Regularities of Thin Ferrofluid Layer Manipulated by Vertical Magnetic Field. *J. Wuhan Univ. Technol.* 34 (01), 10–14. doi:10.1007/s11595-019-2006-1

Chen, M. J., Shen, H., and Li, X. (2016). Magnetic Fluids' Stability Improved by Oleic Acid Bilayer-Coated Structure via One-Pot Synthesis. *Chem. Pap.* 70 (12), 1642–1648. doi:10.1515/chempap-2016-0096

Colla, L., Fedele, L., Scattolini, M., and Bobbo, S. (2012). Water-Based Fe2O3 Nanofluid Characterization: Thermal Conductivity and Viscosity Measurements and Correlation. *Adv. Mech. Eng.* 4, 674947–675298. doi:10.1155/2012/674947

Dong, Y., Wen, B., Chen, Y., Cao, P., and Zhang, C. (2016). Autoclave-free Facile Approach to the Synthesis of Highly Tunable Nanocrystal Clusters for Magnetic Responsive Photonic Crystals. *RSC Adv.* 6, 64434–64440. doi:10.1039/C6RA10355C

Fannin, P. C., and Charles, S. W. (2001). A Comparative Study of the Determination of Ferrofluid Particle Size by Means of Rotational Brownian Motion and Translational Brownian Motion. *Czech. J. Phys.* 51, 599–608. doi:10.1023/A:1017508620729

Iskander, T. (2021). Impact of thermal Conductivity on the Thermophysical Properties and Rheological Behavior of Nanofluid and Hybrid Nanofluid. *Math. Sci.*, 1–9. doi:10.1007/s40096-021-00377-6

Jia, B., and Gao, L. (2007). Fabrication of Fe3O4 Core-Shell Polyhedron Based on a Mechanism Analogue to Ostwald Ripening Process. *J. Cryst. Growth* 303, 616–621. doi:10.1016/j.jcrysgro.2007.01.023

Jun, Y.-W., Huh, Y.-M., Choi, J.-S., Lee, J.-H., Song, H.-T., Kim, S., et al. (2005). Nanoscale Size Effect of Magnetic Nanocrystals and Their Utilization for Cancer Diagnosis via Magnetic Resonance Imaging. *J. Am. Chem. Soc.* 127 (16), 5732–5733. doi:10.1021/ja0422155

Kamali, S., Pouryazdan, M., Ghafari, M., Itou, M., Rahman, M., Stroeve, P., et al. (2016). Magnetization and Stability Study of a Cobalt-Ferrite-Based Ferrofluid. *J. Magnetism Magn. Mater.* 404, 143–147. doi:10.1016/j.jmmm.2015.12.007

Khan, S. U., Al-Khaled, K., Aldabesh, A., Awais, M., and Tlili, I. (2021). Bioconvection Flow in Accelerated Couple Stress Nanoparticles with Activation Energy: Bio-Fuel Applications. *Sci. Rep.* 11, 3331. doi:10.1038/s41598-021-82209-0

Lemes, M. A., Rabelo, D., and Elcana de Oliveira, A. (2017). A Novel Method to Evaluate Nanofluid Stability Using Multivariate Image Analysis. *Anal. Methods* 9, 5826–5833. doi:10.1039/C7AY00645D

Li, J., Li, D., Zhang, S., Cui, H., and Wang, C. (2011). Analysis of the Factors Affecting the Magnetic Characteristics of Nano-Fe3O4 Particles. *Chin. Sci. Bull.* 56, 803–810. doi:10.1007/s11434-010-4126-z

Li, Q., Xuan, Y., and Li, B. (2007). Simulation and Control Scheme of Microstructure in Magnetic Fluids. *Sci. China Ser. E* 50, 371–379. doi:10.1007/s11431-007-0037-x

López-López, M. T., Gómez-Ramírez, A., Rodríguez-Arco, L., Durán, J. D. G., Iskakova, L., and Zubarev, A. (2012). Colloids on the Frontier of Ferrofluids. Rheological Properties. *Langmuir* 28, 6232–6245. doi:10.1021/la204112w

Ma, M., Zhang, Y., Yu, W., Shen, H.-y., Zhang, H.-q., and Gu, N. (2003). Preparation and Characterization of Magnetite Nanoparticles Coated by Amino Silane. *Colloids Surf. A: Physicochemical Eng. Aspects* 212, 219–226. doi:10.1016/S0927-7757(02)00305-9

Mabood, F., and Akinshilo, A. T. (2021). Stability Analysis and Heat Transfer of Hybrid Cu-Al2O3/H2O Nanofluids Transport over a Stretching Surface. *Int. Commun. Heat Mass Transfer* 123, 105215. doi:10.1016/j.icheatmasstransfer.2021.105215

Mahbubul, I. M. (2019). *Stability and Dispersion Characterization of Nanofluid. Preparation, Characterization, Properties and Application of Nanofluid.* London: Applied Science Publishers, 47–112. doi:10.1016/B978-0-12-813245-6.00003-4

Mathew, D. S., and Juang, R.-S. (2007). An Overview of the Structure and Magnetism of Spinel Ferrite Nanoparticles and Their Synthesis in Microemulsions. *Chem. Eng. J.* 129, 51–65. doi:10.1016/j.cej.2006.11.001

Nayak, M. K., Mabood, F., Tlili, I., Dogonchi, A. S., and Khan, W. A. (2020). Entropy Optimization Analysis on Nonlinear thermal Radiative Electromagnetic Darcy-Forchheimer Flow of SWCNT/MWCNT Nanomaterials. *Appl. Nanosci.* 11 (6), 399–418. doi:10.1007/s13204-020-01611-8

Nishio, K., Ikeda, M., Gokon, N., Tsubouchi, S., Narimatsu, H., Mochizuki, Y., et al. (2007). Preparation of Size-Controlled (30-100nm) Magnetite Nanoparticles for Biomedical Applications. *J. Magnetism Magn. Mater.* 310, 2408–2410. doi:10.1016/j.jmmm.2006.10.795

Ozel, F., Kockar, H., and Karaagac, O. (2015). Growth of Iron Oxide Nanoparticles by Hydrothermal Process: Effect of Reaction Parameters on the Nanoparticle Size. *J. Supercond. Nov. Magn.* 28, 823–829. doi:10.1007/s10948-014-2707-9

Poddar, P., Srikanth, H., Morrison, S. A., and Carpenter, E. E. (2005). Inter-particle Interactions and Magnetism in Manganese-Zinc Ferrite Nanoparticles. *J. Magnetism Magn. Mater.* 288, 443–451. doi:10.1016/j.jmmm.2004.09.135

Shahrul, I. M., Mahbubul, I. M., Saidur, R., and Sabri, M. F. M. (2016). Experimental Investigation on Al2O3-W, SiO2-W and ZnO-W Nanofluids and Their Application in a Shell and Tube Heat Exchanger. *Int. J. Heat Mass Transfer* 97, 547–558. doi:10.1016/j.ijheatmasstransfer.2016.02.016

Shahsavar, A., Salimpour, M. R., Saghafian, M., and Shafii, M. B. (2016). Effect of Magnetic Field on thermal Conductivity and Viscosity of a Magnetic Nanofluid Loaded with Carbon Nanotubes. *J. Mech. Sci. Technol.* 30, 809–815. doi:10.1007/s12206-016-0135-4

Sharifi, I., Shokrollahi, H., and Amiri, S. (2012). Ferrite-based Magnetic Nanofluids Used in Hyperthermia Applications. *J. Magnetism Magn. Mater.* 324 (6), 903–915. doi:10.1016/j.jmmm.2011.10.017

Socoliuc, V.-M., and Vékás, L. (2014). Hydrophobic and Hydrophilic Magnetite Nanoparticles: Synthesis by Chemical Coprecipitation and Physico-Chemical Characterization. *Upscaling of Bio-Nano-Processes* 10, 39–55. doi:10.1007/978-3-662-43899-2_3

Sugimoto, T., Wang, Y., Itoh, H., and Muramatsu, A. (1998). Systematic Control of Size, Shape and Internal Structure of Monodisperse α-Fe2O3 Particles. *Colloids Surf. A: Physicochemical Eng. Aspects* 134, 265–279. doi:10.1016/S0927-7757(97)00103-9

Tang, H. (2011). Particle Size Polydispersity of the Rheological Properties in Magnetorheological Fluids. *Sci. China Phys. Mech. Astron.* 54, 1258–1262. doi:10.1007/s11433-011-4355-4

Tang, Z. X., Sorensen, C. M., Klabunde, K. J., and Hadjipanayis, G. C. (1991). Size-dependent Curie Temperature in nanoscaleMnFe2O4particles. *Phys. Rev. Lett.* 67, 3602–3605. doi:10.1103/PhysRevLett.67.3602

Tlili, I., Samrat, S. P., and Sandeep, N. (2021). A Computational Frame Work on Magnetohydrodynamic Dissipative Flow over a Stretched Region with Cross Diffusion: Simultaneous Solutions. *Alexandria Eng. J.* 60, 3143–3152. doi:10.1016/j.aej.2021.01.052

Vasilescu, C., Latikka, M., Knudsen, K. D., Garamus, V. M., Socoliuc, V., Turcu, R., et al. (2018). High Concentration Aqueous Magnetic Fluids: Structure, Colloidal Stability, Magnetic and Flow Properties. *Soft Matter* 14, 6648–6666. doi:10.1039/C7SM02417G

Wang, W., Chen, X., Cai, Q., Mo, G., Jiang, L. S., Zhang, K., et al. (2008). *In Situ* SAXS Study on Size Changes of Platinum Nanoparticles with Temperature. *Eur. Phys. J. B* 65 (1), 57–64. doi:10.1140/epjb/e2008-00322-7

Yadav, D., Bhargava, R., and Agrawal, G. S. (2013). Thermal Instability in a Nanofluid Layer with a Vertical Magnetic Field. *J. Eng. Math.* 80, 147–164. doi:10.1007/s10665-012-9598-1

Yang, S., Sun, Y., Chen, L., Hernandez, Y., Feng, X., and Müllen, K. (2012). Porous Iron Oxide Ribbons Grown on Graphene for High-Performance Lithium Storage. *Sci. Rep.* 2, 427. doi:10.1038/srep00427

Yang, X., Zhang, Z., and Li, D. (2013). Numerical and Experimental Study of Magnetic Fluid Seal with Large Sealing gap and Multiple Magnetic Sources. *Sci. China Technol. Sci.* 56, 2865–2869. doi:10.1007/s11431-013-5365-4

Conflict of Interest: The authors declare that the research was conducted in the absence of any commercial or financial relationships that could be construed as a potential conflict of interest.

Publisher's Note: All claims expressed in this article are solely those of the authors and do not necessarily represent those of their affiliated organizations, or those of the publisher, the editors and the reviewers. Any product that may be evaluated in this article, or claim that may be made by its manufacturer, is not guaranteed or endorsed by the publisher.